

Synthesis of Metal Chalcogenide Semiconductors by Thermal Decomposition of Organosulfur and Organoselenium Compounds

Special
CollectionKeisuke Obata,^[a] Tomohiro Higashi,^[b] Motoki Hasegawa,^[a] Masao Katayama,^[a, c] and Kazuhiro Takanabe*^[a]

Abstract: Metal chalcogenides – because of their excellent optical and electrical properties – are important semiconductor materials for optical devices, such as solar cells, sensors, and photocatalysts. The challenges associated with metal chalcogenides are the complexity of the conventional synthesis methods and the stringent synthesis conditions. In this study, the synthesis conditions were simplified in a solvent-free synthesis method using cadmium precursor, thiourea and selenium to synthesize metal chalcogenides, such as CdS and CdSe, which have particularly suitable band gaps for the

optical devices. CdS_xSe_{1-x} solid solution was successfully synthesized under molten thiourea as the reactive reaction medium at relatively low temperatures, even at 180 °C, with residual melamine derivatives in the solid phase. The luminescence properties of CdS_xSe_{1-x} and the products in the gas and solid phases were investigated. Optimization of the synthesis conditions for solid solutions of CdS_xSe_{1-x} and the role of organic compounds in the formation of metal chalcogenides are discussed.

Introduction

II–VI semiconductors, such as oxides, sulfides, selenides, and tellurides, have attracted great interest in the past few decades due to their unique optical, electrical, and catalytic properties. These properties have also made them candidate materials for solar cells, photocatalysts, thin-film transistors, sensors, photo-detectors, and non-volatile memory devices. CdS_xSe_{1-x}, a solid solution of CdS and CdSe, has the following strengths when used in the above applications; tunable band gap, light emission, and high light absorption coefficient in the visible and infrared region. Because CdS and CdSe have wurtzite and

sphalerite type crystalline structures, the CdS_xSe_{1-x} solid solution can have a crystalline structure of either of them depending on their substitution level.^[1–3] The conduction band and valence band in CdS are constituted by (Cd 5s + S 3p) and S 3p, respectively.^[4] When Se is substituted for S in CdS, the valence band shift towards the vacuum level due to the introduction of Se 4p to S 3p. Unique properties are often introduced through quantum confinement and dimensionality dependence,^[5,6] such as zero-dimension (quantum dots),^[7] one-dimension (nanowire and nanorods),^[8,9] and two-dimension (nanosheets and nanoribbons).^[10,11]

Various synthetic methods have been developed, such as hot injection,^[12–14] vapor deposition,^[15,16] and electrodeposition.^[17,18] However, these methods often have disadvantages, such as a high amount of hazardous waste liquid, high preparation cost, and large energy consumption. Inexpensive and solvent-free synthesis of mixed metal chalcogenides is of great interest for macroelectronics, optoelectronics, photovoltaics, and photocatalysts. In general, solid-state synthesis requires specific precursors for metal chalcogenides and very high temperatures, often under vacuum and sealed conditions.^[19,20] Methods using thiourea as a precursor for sulfur are often utilized. The nucleation and growth of the chalcogenide crystalline are highly dependent on the conversion kinetics of the precursors.^[21,22] Unlike the synthesis in the solution phase, the reaction intermediates are immobile in the solid state, so the reaction mechanisms involved are expected to differ.

Recently, our research group reported a facile method to synthesize metal sulfides at relatively low temperatures (300 °C) in a semi-closed crucible using metal oxides or nitrates and thiourea as the precursors.^[23] This synthetic method has been reported to be able to synthesize first-row transition metal

[a] Dr. K. Obata, M. Hasegawa, Prof. M. Katayama, Prof. K. Takanabe
Department of Chemical System Engineering, School of Engineering
The University of Tokyo
7-3-1 Hongo, Bunkyo-ku, Tokyo, 113-8656 (Japan)
E-mail: takanabe@chemsys.t.u-tokyo.ac.jp

[b] Dr. T. Higashi
Institute for Tenure Track Promotion
University of Miyazaki
Nishi 1–1 Gakuen-Kibanadai, Miyazaki, 889-2192 (Japan)

[c] Prof. M. Katayama
Environmental Science Center
The University of Tokyo
7-3-1, Hongo, Bunkyo-ku, Tokyo 113-0033 (Japan)

Supporting information for this article is available on the WWW under <https://doi.org/10.1002/chem.202201951>

This manuscript is part of a Special Collection “Brightening the Future with Photocatalysis”.

© 2022 The Authors. Chemistry - A European Journal published by Wiley-VCH GmbH. This is an open access article under the terms of the Creative Commons Attribution Non-Commercial NoDerivs License, which permits use and distribution in any medium, provided the original work is properly cited, the use is non-commercial and no modifications or adaptations are made.

sulfide as binary chalcogenides and more complex quaternary metal sulfides, $\text{CuGa}_2\text{In}_3\text{S}_8$ (CGIS), without the use of any solvent.^[23] Thiourea becomes a molten salt at 182 °C, acting as a solvent for the metal precursor. It has both a hard base, NH_2 , and a soft base, S in thione, which can react with metal sources based on Lewis acidity and provide the sulfur source.^[24,25] This solid-phase precursor synthesis, which eventually becomes a molten state, is very simple and can be performed in the air without sealing, making it a useful synthesis compared to the conventional sulfidation. Although thermal decomposition of thiourea has been discussed,^[26] the details of the reaction between the metal precursor and thiourea in this method have not yet been reported, and the reason why the reaction proceeds at a relatively low temperature compared to the conventional solid-phase method is not yet known.

This study investigated the solvent-free synthesis of metal chalcogenide semiconductors using the thermal decomposition of organosulfur and organoselenium compounds. Among the metal chalcogenide semiconductors, we focused on CdS, CdSe, and their solid solutions because these have high absorption coefficients and luminescence properties in the visible light region, and their band gaps can be tuned easily. In addition, understanding the sulfurization reaction, which proceeds under relatively mild conditions, is important for developing various applications. The detailed mechanisms of these reactions involved in this unique synthesis will be discussed to establish universal synthetic protocols for various chalcogenide materials.

Results and Discussion

Synthesis of Cd chalcogenides

First, we attempted to synthesize Cd chalcogenides using various precursors, as summarized in Table 1, following the heating process previously reported.^[23] First, pure CdS and CdSe can be obtained by using thiourea and selenourea, respectively, at 300 °C in the air indicating chalcogen-based urea as a promising precursor for the synthesis of chalcogenides (entry 1 and 2 in Table 1, Figure S1). Their crystalline structures were a

hexagonal wurtzite and a cubic sphalerite for CdS and CdSe, respectively. It is well known that these phases can be formed in the chalcogenides depending on the synthesis temperature and the precursors.^[27–30] Phase transition from the sphalerite to the wurtzite is reported to occur at 300 °C.^[27,28] We suspect that our synthesis temperature is close to the critical temperature resulting in the different crystalline structure. An excess urea source seems to be required to synthesize the chalcogenides without remaining CdO (Figure S1). However, $\text{CdS}_x\text{Se}_{1-x}$ solid solution was not obtained, and CdSe was preferentially formed when these precursors were used together (entry 3–5 in Table 1, Figure S2).

$\text{CdS}_x\text{Se}_{1-x}$ solid solution was successfully obtained when Se metal powder or SeO_2 were used as the Se source (entries 6 and 7 in Table 1, Figure 1 and Figure S3). Selenide seems to be introduced more preferably when Se powder is used as the Se source. Prolonged reaction time using SeO_2 did not increase the adsorption edge further indicating that the reaction was completed within 12 h (Figure S3b). The difference of selenization between the Se sources, Se powder and SeO_2 , may be due to the amount of reducing agents required for the selenide formation. Se^{4+} in SeO_2 has to be reduced to Se^{2-} while Se^0 in Se powder needs to be reduced to Se^{2-} before the compound formation. Various Cd and S sources have also been tried (entries 8–12, Figure S4 and S5). Only cadmium acetate as the Cd source produced the $\text{CdS}_x\text{Se}_{1-x}$ solid solution like CdO. Indeed, cadmium acetate is often used as a precursor to synthesize CdSe quantum dots.^[31–33] Other Cd sources did not show any notable shift of the absorption edge, which may reflect the Cd precursors' stability and coordination strength. Methylthiourea can also be used as an S source (entry 12 in Table 1, Figure S5). However, its absorption edge wavelength was lower than that prepared from thiourea (Figure S5b), indicating that selenization is insufficient in molten methylthiourea, which has a melting temperature of 120 °C. Based on the screening above, the precursors shown in entry 6 are used as the standard precursors in the following discussion. Notably, $\text{CdS}_x\text{Se}_{1-x}$ was obtained by heating at an even lower temperature, 180 °C, indicating a unique function of thiourea as a molten solvent (Figure S6a and b). It also must be noted that

Table 1. Summary for the synthesis of Cd chalcogenides with various precursors. Heat treatment was performed at 300 °C for 12 h in air. The precursors were Cd source 1 mmol, S source 2 mmol, and Se source 0.5 mmol unless otherwise specified. The standard precursors used in the following discussion are shown in bold.

Entry	Cd source	S source	Se source	Obtained material
1	CdO	Thiourea	–	CdS (Figure S1)
2	CdO	–	Selenourea	CdSe (Figure S1)
3	CdS ^[a]	–	Selenourea	Mixture of CdS and CdSe (Figure S2)
4	CdSe ^[b]	Thiourea 1.5 mmol	–	CdSe (Figure S2)
5	CdO	Thiourea	Selenourea	CdSe (Figure S2)
6	CdO	Thiourea	Se	$\text{CdS}_x\text{Se}_{1-x}$ (Figure 1, Figure S3)
7	CdO	Thiourea	SeO_2	$\text{CdS}_x\text{Se}_{1-x}$, the absorption edge is lower than entry 6 (Figure S3)
8	$\text{Cd}(\text{CH}_3\text{COO})_2 \cdot 2\text{H}_2\text{O}$	Thiourea	Se 0.3 mmol	$\text{CdS}_x\text{Se}_{1-x}$ (Figure S4)
9	$\text{Cd}(\text{NO}_3)_2 \cdot 4\text{H}_2\text{O}$	Thiourea	Se 0.3 mmol	CdS (Figure S4)
10	$\text{CdSO}_4 \cdot 8\text{H}_2\text{O}$	Thiourea	Se 0.3 mmol	CdS (Figure S4)
11	$\text{CdCl}_2 \cdot 2.5\text{H}_2\text{O}$	Thiourea	Se 0.3 mmol	Various byproducts (Figure S4)
12	CdO	Methylthiourea	Se	$\text{CdS}_x\text{Se}_{1-x}$, the absorption edge is lower than entry 6 (Figure S5)

[a] Synthesized by entry 1. [b] Synthesized by entry 2.

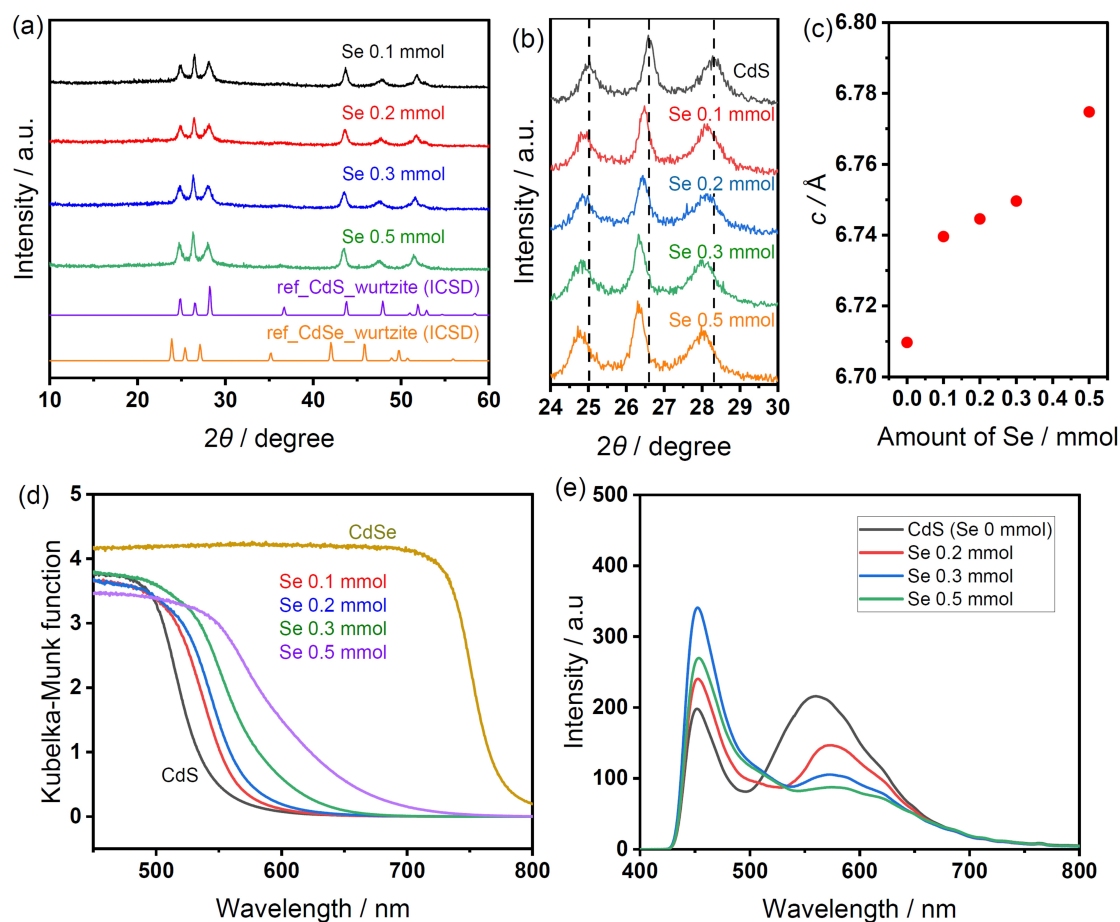


Figure 1. (a,b) XRD patterns, (c) Lattice constant estimated from 2θ value at (002), (d) UV-vis DRS spectra, and (e) photoluminescent spectra of CdS_{*x*}Se_{1-*x*} solid solution prepared at 300 °C in the air using precursors shown in entry 6 in Table 1 with various amounts of Se.

CdS_{*x*}Se_{1-*x*} solid solution was obtained irrespective of the surrounding gas atmosphere, either Ar or air (Figure S6c and d), demonstrating its facile synthesis compared to the previously reported sulfurization method using a vacuum-sealed quartz tube at high temperature.^[34]

CdS_{*x*}Se_{1-*x*} solid solution synthesized by entry 6 in Table 1 with various Se content was further characterized. As shown in the XRD patterns in Figure 1a and b, the prepared CdS_{*x*}Se_{1-*x*} solid solution has the wurtzite structure in the present substitution range. X-ray diffraction (XRD) peaks for (101) at 28°, (002) at 26.5°, and (100) at 25° shifted negatively (Figure 1b), indicating the lattice expansion (Figure 1c) and the successful substitution of Se, which has a larger ionic radius, in the S site. According to Vegard's law [Equation (1)], 35% of S is substituted by Se when 0.5 mmol of Se powder is added to the precursors.

$$a_{\text{CdS}_x\text{Se}_{1-x}} = xa_{\text{CdS}} + (1-x)a_{\text{CdSe}} \quad (1)$$

UV-vis diffuse reflectance spectroscopy (DRS) spectra also confirm the formation of CdS_{*x*}Se_{1-*x*} solid solution (Figure 1d). Pure CdS shows an absorption edge wavelength of 520 nm, corresponding to the band gap of 2.4 eV.^[3] With increasing the

amount of Se powder (0.1–0.5 mmol) in the precursors, the absorption edge shifted to the longer wavelength and was located between pure CdS and commercial CdSe, which indicates the successful formation of the CdS_{*x*}Se_{1-*x*} solid solution. The absorption edge shifts because the position of the valence band gets shallower than that of the pure S 3p orbital due to the hybridization of the S 3p and Se 4p orbitals. Figure 1e shows the photoluminescence (PL) spectra of CdS_{*x*}Se_{1-*x*}. The peak between 550 and 600 nm is the emission of Cd chalcogenides, which shifts to a longer wavelength as the amount of Se in the precursors increases. The peak intensity in this region decreases by the substitution because the emission intensity of CdSe is lower than that of CdS.^[35] The emission peak located at 450 nm originates from the surface S defect.^[35] By adding Se in the precursor, the peak intensity at 450 nm increases, suggesting that the amount of surface defect increased. A photocatalytic activity test was also conducted in the presence of electron donors, Na₂S and NaSO₃, after loading the Pt co-catalyst (Figure S7). Continuous production of H₂ was observed under light irradiation. The apparent quantum efficiency (AQY) was 0.4% at 420 nm for CdS without Se substitution. However, the production rate of H₂ and AQY dropped by adding the Se in the precursor, although the light

absorption edge shifted to a higher wavelength. This is likely because of bulk or surface defects observed in PL spectra, which need to be overcome in future work to achieve photocatalytic H₂ production efficiently under visible light irradiation. All the characterizations mentioned above support the successful formation of the CdS_xSe_{1-x} solid solution. The reaction mechanism during the synthesis is further discussed in the following sections.

Analysis during the synthesis of chalcogenides

Figures 2a and b show thermogravimetry – differential thermal analysis (TG-DTA) curves of the pure thiourea and the precursor mixture, respectively, heated in air. First, endothermic peaks located at 180 °C in Figure 2a are assigned to the melting of thiourea. After melting, thiourea and ammonium thiocyanate form an equilibrium mixture.^[26] The second peak at 220 °C comes from their thermal decomposition to gaseous products, such as NH₃, HNCS, CS₂, and H₂NCN, leading to mass loss.^[26] Organic residues, such as melam, melem, and C₃N₄, are expected to remain in the solid phase until the temperature is elevated to 600 °C. When CdO and Se powder are added to thiourea (Fig 2b), new exothermic peaks appear in addition to the above-mentioned endothermic peaks coming from the melting and the thermal decomposition of thiourea. The exothermic peak at 200 °C can be assigned to the substitution reaction of S and Se in CdO, considering the thermodynamics and synthesis shown in Figures S6a and S6b. These results indicate that the formation of CdS_xSe_{1-x} solid solution occurs in the molten thiourea as a reaction media in a mild heating

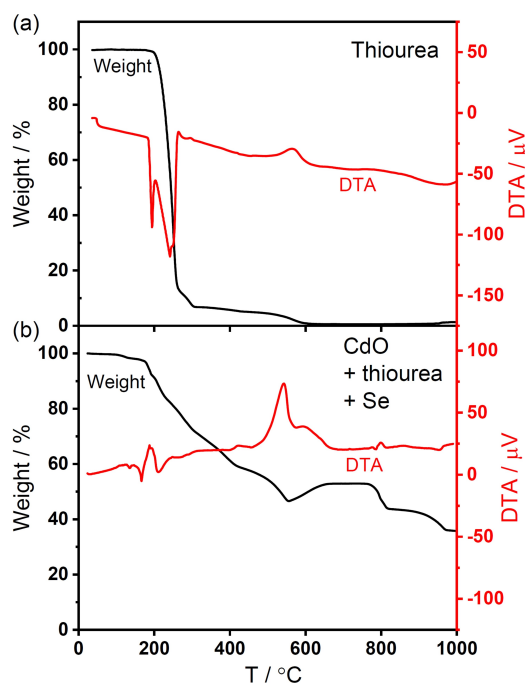


Figure 2. TG-DTA curves of (a) thiourea and (b) mixture of CdO, thiourea, Se powder (CdO:thiourea:Se = 1:2:0.3).

condition. The peaks between 500 and 700 °C come from the oxidation of chalcogenide by heating in the air.

The gaseous products during the synthesis were analyzed by a mass spectrometer (MS) for the pure thiourea and the precursor mixture, as shown in Figure 3. First, various gaseous products were observed from the thiourea above 220 °C (Figure 3a), which agrees with its thermal decomposition observed in TG-DTA (Fig 2a). Notably, NH₃ and H₂O were the only gaseous products when the precursor mixture was heated together, suggesting that carbon and chalcogen remained in the solid phase. H₂O and NH₃ are expected to be formed during sulfurization of CdO and amine condensation of melamine derivatives, respectively, which will be discussed later. Organic elemental analysis (OEA) was conducted on the samples after heat treatment (Table 2) to determine whether organic residues remained in the solid phase. The C:N molar ratio should be 1:2, 1:1.83, 1:1.66, and 1:1.33 for melamine, melam, melem, and carbon nitride, respectively, which are expected to be formed from cyanamide. The main organic residues seem to be melem

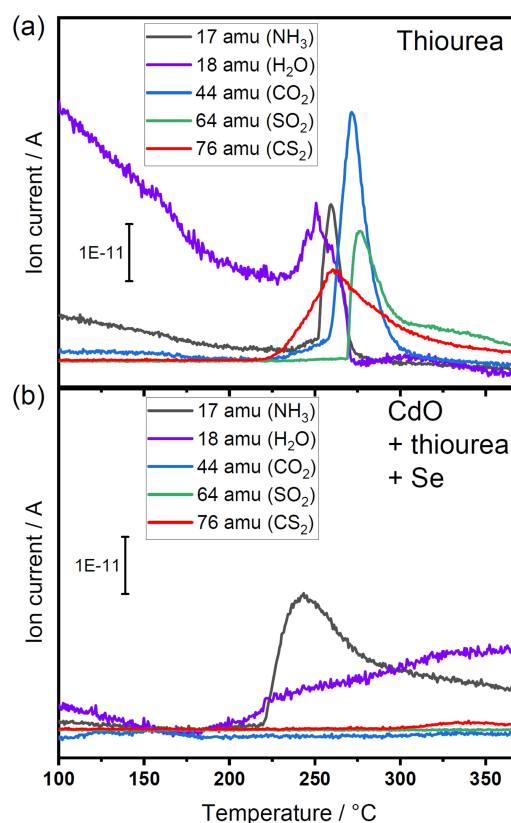


Figure 3. Mass spectrometric (MS) signals were obtained by heating (a) thiourea and (b) a mixture of CdO, thiourea, and Se powder (CdO:thiourea:Se = 1:1:0.3) at 10 °C min⁻¹ with the flow of air at 100 mL min⁻¹.

Table 2. OEA results of samples after synthesis at 190 and 300 °C. The precursor was 1 mmol CdO, 2 mmol thiourea and 0.5 mmol Se powder.

Heating temperature/[°C]	C:N (molar ratio)	Carbon weight/[g]
190	1:1.69	0.028
300	1:1.48	0.025

after heating at 190 °C, while the mixture of melam and carbon nitride is the major organic product in the sample synthesized at 300 °C. The decrease of the C:N ratio at elevated temperature suggests the successive amine condensation of melamine leading to the formation of its derivatives and gaseous NH₃ as observed in TG-DTA and MS signals (Figure 2b and Figure 3b). The weight of carbon in the precursor mixture before heating was 0.024 g, which remained unchanged after the synthesis, indicating that carbon in the precursor remained in the solid phase. Indeed, an amorphous shell composed of carbon was also observed around the chalcogenide in the TEM image (Figure S8). Melamine derivatives, such as graphitic carbon nitride and amorphous carbon nitride, are reported to have bandgap of 2.8 and 1.9 eV, respectively, which may influence the photocatalytic activity.^[36] In our study, the organic residue seems to be amorphous as shown in Figure S8. However, absorption corresponding to amorphous carbon nitride (680 nm) was not observed (Figure 1d). Furthermore, in our photocatalytic tests with various Se contents (Figure S7), there was a clear difference on the activity although the same amount of thiourea was introduced, which indicates that organic residue in our study has a negligible impact on the observed photocatalytic activity. The reason would be low degree of polymerization and incomplete formation of electronic band structure due to the synthesis at moderate temperature (300 °C).^[37,38] To obtain appreciable photocatalytic activity from the melamine derivatives, synthesis temperature needs to be elevated (650 °C)^[37] while maintaining the chalcogenides.

Based on the above-mentioned characterizations, Scheme 1 shows the plausible formation pathway of the chalcogenides and the organic residues. CdO and thiourea first form the chalcogenide and the cyanamide in a molten solid phase, and the gaseous H₂O is produced above 190 °C. The cyanamide undergoes the polymerization to form the melamine, followed by the amine condensation producing the gaseous NH₃ and melam derivatives in the solid phase. The condensation continues until it forms graphitic carbon nitride. Scheme 1 just shows the sulfurization of CdO using thiourea. To form CdS_xSe_{1-x} solid solution, Se metal powder or SeO₂ (entry 7 in Table 1) must be reduced to selenide. Although Se and SeO₂ are often used as the Se source to form CdSe quantum dots, its transformation to selenide often remains unclear.^[39] Hydrazine, NaBH₄, ascorbic acid, and mercaptopropionic acid are sug-

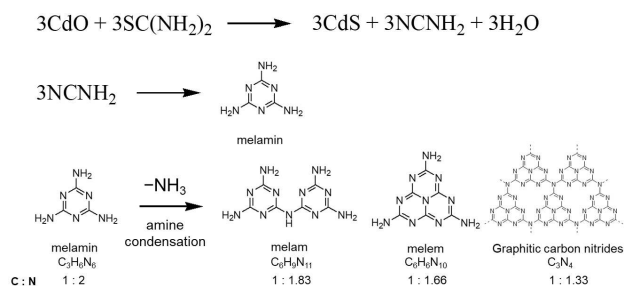
gested to be reducing agents during CdSe synthesis.^[40–43] In the same way, part of the present precursors might have worked as a reducing agent, which we keep beyond the scope of this study. Finally, organic residue coming from the melamine derivatives needs to be removed from the chalcogenides depending on their applications. Although decomposition of graphitic carbon nitride is known to occur above 550 °C in air,^[37] this condition may trigger the oxidation of chalcogenides as well (Figure 2b). Heat treatment alone may not be an effective approach. Alternatively, carbon nitride can be oxidized by photogenerated holes or OH radicals.^[38,44] However, these approaches may also oxidize the chalcogenides. Since the graphitic carbon nitride is known to be exfoliated in liquid phase by ultrasonication due to its weak Van der Waals interaction,^[45] we propose to transform the organic residue to the graphitic carbon nitride in moderate temperature (< 500 °C), where the chalcogenides can be maintained, followed by the exfoliation process to disperse the carbon nitride sheets in the liquid phase.

Synthesis of various chalcogenides using thiourea

We have previously demonstrated the sulfurization of the first row transition metal oxides using the present method. Sulfurization for various metal oxides was further explored, as shown in Figure 4. Bi₂S₃ and In₂S₃ have been successfully synthesized (Figure 4b–d), demonstrating that the present method would be a potential option for synthesizing various metal chalcogenides. One of the major reasons to determine the successful synthesis of the sulfides is the thermodynamics (Figure S9). The elements which did not form the corresponding sulfides have positive Gibbs free energy changes (ΔG) in the moderate temperature range in this study suggesting that these oxides are more stable than their sulfides. The exception is the Ga whose ΔG is negative. We suspect that kinetics might be inhibiting the synthesis of Ga₂S₃. We leave further optimization to obtain Ga₂S₃ beyond the scope of this study. Although gallium sulfide was not obtained in this study, complex sulfide, CuGa₂In₃S₈, was synthesized in our previous report,^[23] suggesting a broad possibility to synthesize various chalcogenides.

Conclusion

In the present study, the solvent-free synthesis method using thiourea has been explored to obtain chalcogenide semiconductors. A CdS_xSe_{1-x} solid solution was successfully obtained from the mixture of CdO, thiourea, and Se at a moderate heating condition in the air. The role of thiourea was investigated by various characterizations during the synthesis. It was revealed that the thiourea turns into a molten reaction media above 190 °C, which allows the synthesis of chalcogenide at low temperature while leaving organic residues, such as melamine derivatives and graphitic carbon nitride, in the solid phase. Future studies require effective removal of the organic residues and surface defects depending on their applications.



Scheme 1. Plausible formation pathway of the chalcogenides and the organic residue.

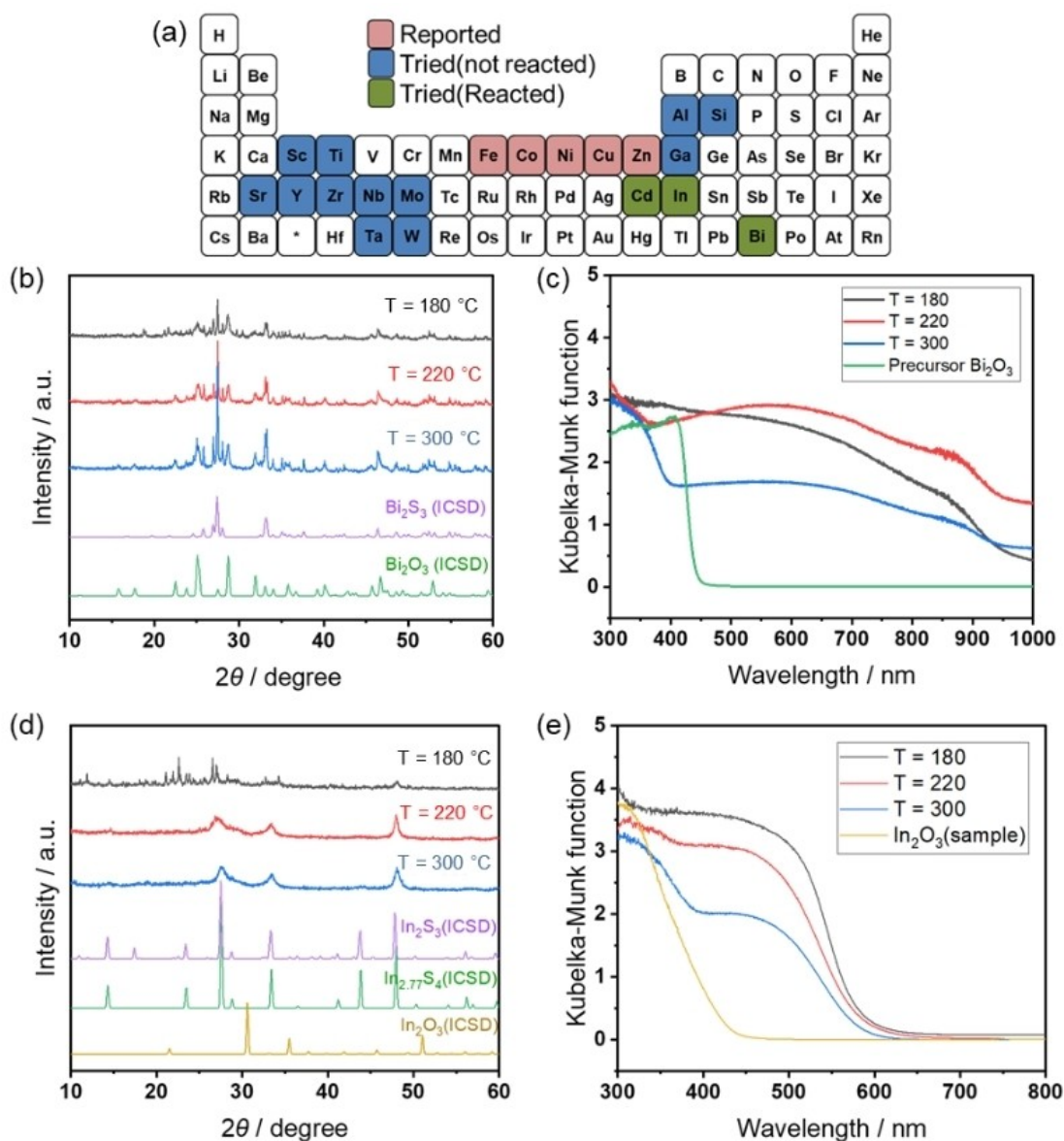


Figure 4. (a) Summary of the sulfurization with various elements using thiourea. (b,d) XRD patterns, (c,e) UV-vis DRS spectra of samples synthesized at various temperatures in air for 12 h with thiourea (16 mmol), and (b,c) Bi₂O₃ (1 mmol) or (d,e) In₂O₃ (1 mmol).

Experimental Section

Chemicals: All the chemicals were used as received. CdO (99%, Strem Chemical, Inc.), Cd(CH₃COO)₂·2H₂O (99.9%, FUJIFILM Wako Pure Chemical Corp.), Cd(NO₃)₂·4H₂O (99%, Strem Chemical, Inc.), CdSO₄·8H₂O (≥ 99.99%, Merck Sigma-Aldrich), CdCl₂·2.5H₂O (99.9%, FUJIFILM Wako Pure Chemical Corp.), thiourea (≥ 99.0%, Merck Sigma-Aldrich), methylthiourea (≥ 98.0%, Tokyo Chemical Industry Co.), selenourea (95.0+%, FUJIFILM Wako Pure Chemical Corp.), selenium (99.9+%, FUJIFILM Wako Pure Chemical Corp.), SeO₂ (97%, FUJIFILM Wako Pure Chemical Corp.), Bi₂O₃ (99.9%, FUJIFILM Wako Pure Chemical Corp.), and In₂O₃ (99.9%, FUJIFILM Wako Pure Chemical Corp.).

Synthesis of chalcogenides: Precursors were mixed and ground in a mortar and pestle, placed in an alumina crucible, and then heated in a muffle furnace at a given temperature in air for 12 h with a temperature rise of 10 °C min⁻¹.

Powder X-ray diffraction (XRD): XRD measurements were performed using Rigaku RINT-Ultima3 high-resolution X-ray diffraction and small-angle scattering system with a Cu K α X-ray source at a voltage of 40 kV and a current of 30 mA.

Ultraviolet-visible absorption spectroscopy (UV-vis): The UV-visible absorption spectra of the powder were measured using a UV-visible near-infrared spectrophotometer (Japan Spectroscopic V-770). The sample was placed in a dedicated cell, and the intensity of the reflected light at each wavelength was measured using an integrating sphere.

Thermogravimetry-differential thermal analysis (TG-DTA): SHIMADZU DTG-60H were used to obtain the TG and DTA curves of the samples. A platinum pan was used as a container, and an empty container was used as reference material.

Photoluminescence (PL): The photoluminescence spectra of the powders were measured using a spectrophotometer (Japan Spectroscopy FP-8500).

Organic element analyzer (OEA): The presence ratio analysis of C, H, and N of the organic residues in the samples was performed using CE-440F (Exeter Analytical, Inc). The samples were completely combusted in a pure oxygen atmosphere, and the CO₂, H₂O, N₂ and nitrogen oxides produced were quantified.

Mass spectrometry (MS): The decomposition of thiourea was investigated by detecting the products in the gas phase during heating using a mass spectrometer (Transpector CPM). The mass spectrometer was connected to the furnace outlet to study the decomposition products under an airflow of 100 mL min⁻¹ in a temperature range from 20 to 370 °C with a heating rate of 10 °C min⁻¹.

Transmission electron microscope (TEM): The morphology of the samples was characterized using TEM (JEM-2800, JEOL) and scanning transmission electron microscopy (STEM; JEM-2800, JEOL). The STEM was equipped with energy-dispersive X-ray spectroscopy (EDS) capabilities. For TEM sample preparation, a dispersion of the sample in ethanol solvent was drop-casted onto the carbon grid, and it was then dried in air.

Photocatalytic activity test: Prior to the activity test of photocatalytic H₂ production, Pt catalyst was loaded on the synthesized chalcogenides. 100 mg catalyst was dispersed in a mixed solution (Deionized water 5 ml, 1 mg/ml H₂PtCl₆, 19.6 μL), and photodeposition was performed using a 300 W Xe lamp for 30 min. The obtained Pt/CdS_xSe_{1-x} (Pt: 0.1 wt.%) was used in the activity test in a closed circulation system. 50 mg of Pt/CdS_xSe_{1-x} was dispersed in 10 mL of an aqueous solution containing 0.35 M Na₂S and 0.25 M Na₂SO₃ under Ar atmosphere at 21 kPa, and the light was irradiated using a 300 W Xe lamp equipped with UV-vis mirror module and a cut-off filter (420 nm < λ < 600 nm).

Acknowledgements

This work was supported by the Mohammed bin Salman Center for Future Science and Technology for Saudi-Japan Vision 2030 at The University of Tokyo (MbSC2030). The authors are grateful to the Japan Technological Research Association of Artificial Photosynthetic Chemical Process (ARPCHEM) and Prof. K. Domen from the University of Tokyo for providing the selenium and selenourea. We would like to thank Ms. M. Nakabayashi of the University of Tokyo for assisting during the TEM/STEM observation.

Conflict of Interest

The authors declare no conflict of interest.

Data Availability Statement

The data that support the findings of this study are available from the corresponding author upon reasonable request.

Keywords: melamine derivatives · metal chalcogenides · solid solution · solvent-free synthesis · thiourea

- [1] A. S. Hassanien, A. A. Akl, *Superlattices Microstruct.* **2016**, *89*, 153–169.
- [2] K. B. Subila, G. Kishore Kumar, S. M. Shivaprasad, K. George Thomas, *J. Phys. Chem. Lett.* **2013**, *4*, 2774–2779.
- [3] W. Vogel, J. Urban, M. Kundu, S. K. Kulkarni, *Langmuir* **1997**, *13*, 827–832.
- [4] H.-X. Liu, F.-L. Tang, H.-T. Xue, Y. Zhang, Y.-W. Cheng, Y.-D. Feng, *Chin. Phys. B* **2016**, *25*, 123101.
- [5] L. K. Pan, C. Q. Sun, B. K. Tay, T. P. Chen, S. Li, *J. Phys. Chem. B* **2002**, *106*, 11725–11727.
- [6] A. P. Alivisatos, *J. Phys. Chem.* **1996**, *100*, 13226–13239.
- [7] P. Maity, T. Debnath, H. N. Ghosh, *J. Phys. Chem. C* **2015**, *119*, 10785–10792.
- [8] Q. Zhang, H. Liu, P. Guo, D. Li, P. Fan, W. Zheng, X. Zhu, Y. Jiang, H. Zhou, W. Hu, X. Zhuang, H. Liu, X. Duan, A. Pan, *Nano Energy* **2017**, *32*, 28–35.
- [9] G. Dai, H. Zou, X. Wang, Y. Zhou, P. Wang, Y. Ding, Y. Zhang, J. Yang, Z. L. Wang, *ACS Photonics* **2017**, *4*, 2495–2503.
- [10] L. Gundlach, P. Piotrowiak, *J. Phys. Chem. C* **2009**, *113*, 12162–12166.
- [11] X. Zhuang, P. Guo, Q. Zhang, H. Liu, D. Li, W. Hu, X. Zhu, H. Zhou, A. Pan, *Nano Res.* **2016**, *9*, 933–941.
- [12] S. Dey, S. Chen, S. Thota, M. R. Shakil, S. L. Suib, J. Zhao, *J. Phys. Chem. C* **2016**, *120*, 20547–20554.
- [13] D. V. Talapin, J.-S. Lee, M. V. Kovalenko, E. V. Shevchenko, *Chem. Rev.* **2010**, *110*, 389–458.
- [14] G. H. Carey, A. L. Abdelhady, Z. Ning, S. M. Thon, O. M. Bakr, E. H. Sargent, *Chem. Rev.* **2015**, *115*, 12732–12763.
- [15] A. Pan, R. Liu, F. Wang, S. Xie, B. Zou, M. Zacharias, Z. L. Wang, *J. Phys. Chem. B* **2006**, *110*, 22313–22317.
- [16] A. S. Hassanien, A. A. Akl, *J. Alloys Compd.* **2015**, *648*, 280–290.
- [17] M. Hazra, A. Jana, J. Datta, *Appl. Surf. Sci.* **2018**, *454*, 334–342.
- [18] I. M. Dharmadasa, J. Haigh, *J. Electrochem. Soc.* **2006**, *153*, G47.
- [19] I. U. Arachchige, S. L. Brock, *Acc. Chem. Res.* **2007**, *40*, 801–809.
- [20] C. Steinhagen, M. G. Panthani, V. Akhavan, B. Goodfellow, B. Koo, B. A. Korgel, *J. Am. Chem. Soc.* **2009**, *131*, 12554–12555.
- [21] Y. C. Choi, E. J. Yeom, T. K. Ahn, S. I. Seok, *Angew. Chem. Int. Ed.* **2015**, *54*, 4005–4009; *Angew. Chem.* **2015**, *127*, 4077–4081.
- [22] J. van Embden, A. S. R. Chesman, J. J. Jasieniak, *Chem. Mater.* **2015**, *27*, 2246–2285.
- [23] M. K. Bhunia, E. Abou-Hamad, D. H. Anjum, A. Gurinov, K. Takanebe, *Part. Part. Syst. Charact.* **2018**, *35*, 1700183.
- [24] Z. Y. Xu, Y. C. Zhang, *Mater. Chem. Phys.* **2008**, *112*, 333–336.
- [25] C. L. McCarthy, D. H. Webber, E. C. Schueller, R. L. Brutchey, *Angew. Chem. Int. Ed.* **2015**, *54*, 8378–8381; *Angew. Chem.* **2015**, *127*, 8498–8501.
- [26] S. Wang, Q. Gao, J. Wang, *J. Phys. Chem. B* **2005**, *109*, 17281–17289.
- [27] O. Zelaya-Angel, R. Lozada-Morales, *Phys. Rev. B* **2000**, *62*, 13064–13069.
- [28] M. P. Kulakov, I. V. Balyakina, *J. Cryst. Growth* **1991**, *113*, 653–658.
- [29] A. V. Naumov, T. V. Samofalova, V. N. Semenov, I. V. Nechaev, *Russ. J. Inorg. Chem.* **2011**, *56*, 621–627.
- [30] A. V. Naumov, V. N. Semenov, E. G. Goncharov, *Inorg. Mater.* **2001**, *37*, 539–543.
- [31] H. Halim, J. Simon, I. Lieberwirth, V. Mailänder, K. Koynov, A. Riedinger, *J. Mater. Chem. B* **2020**, *8*, 146–154.
- [32] J. Zhang, Y. Sun, S. Ye, J. Song, J. Qu, *Chem. Mater.* **2020**, *32*, 9490–9507.
- [33] A. S. Mule, S. Mazzotti, A. A. Rossinelli, M. Aellen, P. T. Prins, J. C. van der Bok, S. F. Solari, Y. M. Glauser, P. V. Kumar, A. Riedinger, D. J. Norris, *J. Am. Chem. Soc.* **2021**, *143*, 2037–2048.
- [34] G. Ma, Y. Kuang, D. H. K. Murthy, T. Hisatomi, J. Seo, S. Chen, H. Matsuzaki, Y. Suzuki, M. Katayama, T. Minegishi, K. Seki, A. Furube, K. Domen, *J. Phys. Chem. C* **2018**, *122*, 13492–13499.
- [35] X. Ren, Y. Chen, Y. Zhang, L. Wang, *Mater. Sci. Semicond. Process.* **2020**, *105*, 104743.
- [36] Y. Kang, Y. Yang, L.-C. Yin, X. Kang, G. Liu, H.-M. Cheng, *Adv. Mater.* **2015**, *27*, 4572–4577.
- [37] G. Zhang, J. Zhang, M. Zhang, X. Wang, *J. Mater. Chem.* **2012**, *22*, 8083.
- [38] K. Maeda, X. Wang, Y. Nishihara, D. Lu, M. Antonietti, K. Domen, *J. Phys. Chem. C* **2009**, *113*, 4940–4947.
- [39] A. Riedinger, A. S. Mule, P. N. Knüsel, F. D. Ott, A. A. Rossinelli, D. J. Norris, *Chem. Commun.* **2018**, *54*, 11789–11792.
- [40] R. M. Hodlur, M. K. Rabinal, *Chem. Eng. J.* **2014**, *244*, 82–88.

- [41] Y. Wang, M. Yu, K. Yang, J. Lu, L. Chen, *Luminescence* **2015**, *30*, 1375–1379.
- [42] R. Wang, X. Wei, J. Xie, B. Wang, X. He, *Aust. J. Chem.* **2018**, *71*, 524.
- [43] Z. M. S. H. Khan, S. A. Khan, M. Zulfequar, *Mater. Sci. Semicond. Process.* **2017**, *57*, 190–196.
- [44] M. Li, D. Liu, X. Chen, Z. Yin, H. Shen, A. Aiello, K. R. McKenzie, N. Jiang, X. Li, M. J. Wagner, D. P. Durkin, H. Chen, D. Shuai, *Environ. Sci. Technol.* **2021**, *55*, 12414–12423.
- [45] M. I. Chebanenko, N. V. Zakharova, A. A. Lobinsky, V. I. Popkov, *Semiconductors* **2019**, *53*, 2072–2077.

Manuscript received: June 23, 2022
Accepted manuscript online: August 5, 2022
Version of record online: September 1, 2022